Postural Synergies of the UB Hand IV for Human-like Grasping

Fanny Ficuciello[a], Gianluca Palli[b], Claudio Melchiorri[b], Bruno Siciliano[a]

[a] *PRISMA Lab, Dipartimento di Ingegneria Elettrica e Tecnologie dell'Informazione, Università degli Studi di Napoli Federico II, Via Claudio 21, 80125 Napoli, Italy.*
[b] *DEI, Dipartimento di Ingegneria dell'Energia Elettrica e dell'Informazione, Alma Mater Studiorum Università di Bologna, Viale Risorgimento 2, 40136 Bologna, Italy.*

Abstract

In this paper, the postural synergy configuration subspace given by the fundamental eigengrasps of the UB Hand IV is derived from experiments, and a simplified synergy-based strategy for planning grasps is proposed. The objectives of this work are, on one side, the simplification of grasp synthesis in a configuration space of reduced dimensions and, on the other side, the attainment of a human-like behavior for anthropomorphic hands. A reference set of 36 hand postures, chosen with the goal of covering the entire grasp variety referring to a recently proposed taxonomy, has been considered for the evaluation of the hand synergies. With the aim of defining general properties of the three predominant synergies, the reference set of hand postures has been applied to other two anthropomorphic robot hands, and the obtained synergies have been compared with the ones computed considering the UB Hand IV kinematics. Moreover, the synthesis of new grasps, not contained in the reference set of hand postures, has also been achieved by means of the synergy subspace. The experiments carried out demonstrate that the adopted synergy-based planning method works efficiently for all the considered grasps even if not contained in the reference set used for the evaluation of the postural synergies.

Keywords: Grasping, Postural Synergies, Anthropomorphic Robot Hands, Bio-aware Robotics

[☆]This research has been carried out partly within the SAPHARI project funded under grant agreement EU-FP7-ICT-287513, and partly within the RoDyMan project funded by the European Research Council under EU-FP7-ERC Advanced Grant n. 320992.

1. Introduction

In order to interact with humans directly, the robots of the future will require enhanced manipulation capabilities similar to those of human beings. For this purpose, complex dexterous hands with advanced sensorimotor skills and human-like kinematics are needed. The human hand is an excellent example of dexterous bio-mechanical architecture with versatile capabilities to perform different kinds of tasks. The undergoing research in the field aims at the reproduction of human's abilities not only by means of anthropomorphic design but also by adopting human-inspired control strategies. Recent advances in neuroscience have shown that control of the human hand during grasp is dominated by movements in a continuous configuration space of highly reduced dimensionality with respect to the number of DoFs [1], [2]. The goals of this paper are the simplification of grasp synthesis in a configuration space of reduced dimensions and the attainment of a human-like behavior for anthropomorphic hands. In order to allow a direct qualitative comparison with the results obtained on the human hand, the approach reported in [1] has been adopted in this work both for the selection of the posture reference set and for the data analysis. The postural synergies, also

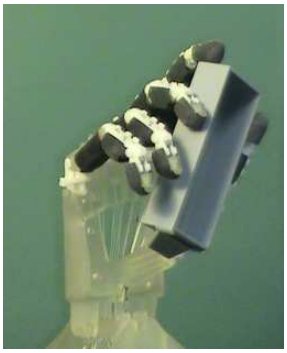

Figure 1: The UB Hand IV prototype.

called simply synergies or eigengrasps, of the UB Hand IV (see Fig. 1) have been derived using the Principal Component Analysis (PCA) by considering a reference set of 36 hand configurations, shown in Fig. 2, divided in four main groups. According to the grasp classification reported in [3], the first three groups of the reference set can be divided in precision, intermediate

and power grasps. Each of these grasps involves objects used in the human everyday life. Since we are interested in planning the whole hand motion during the reach-to-grasp phase and not in describing the grasp only, a fourth group of open hand configurations has been added to the reference set for a complete coverage of the possible hand movements, allowing control of the execution of any grasp. It is worth noticing that considering different relative positions of the object with respect to the hand will result in different grasp configurations and, as a consequence, on different synergies.

The changes in synergies with respect to the change in position and orientation of the objects relative to the palm have not been investigated in this work for three main reasons.

i) Usually humans adapt the hand position with respect to the object before grasping to execute it in a proper way (accordingly also to the task to be performed with the object); hence also for robot hands the grasps can be in some way standardized considering a single object/hand relative position for each grasp, as shown in Fig. 2, and adjusting the hand position before grasp execution.

ii) If the grasp is robust enough (from the point of view of the grasp stability) and the object is not constrained, the hand may change the object position and orientation before the complete grasp is achieved in case one or more fingers contact the object before the others, resulting in an adaptation of the object position to the grasp.

iii) By adopting the synergy-based grasp synthesis, we are not ensured that the location of the contact points, and then the object position too, will be the same considered for synergy derivation; hence constraining the object/hand relative position may result in a degradation of the grasp stability with respect to the case in which an adaptation of the object position by the hand itself during the grasp execution is allowed.

Aiming at the definition of common characteristics of the three predominant synergies, the postural synergies of other two anthropomorphic robot hands, a five-fingered hand with significant differences in the thumb kinematics and a four-fingered hand, have also been evaluated adopting the same posture reference set, and the results obtained from the different kinematic models have been compared. The PCA has been used in this work for synergy

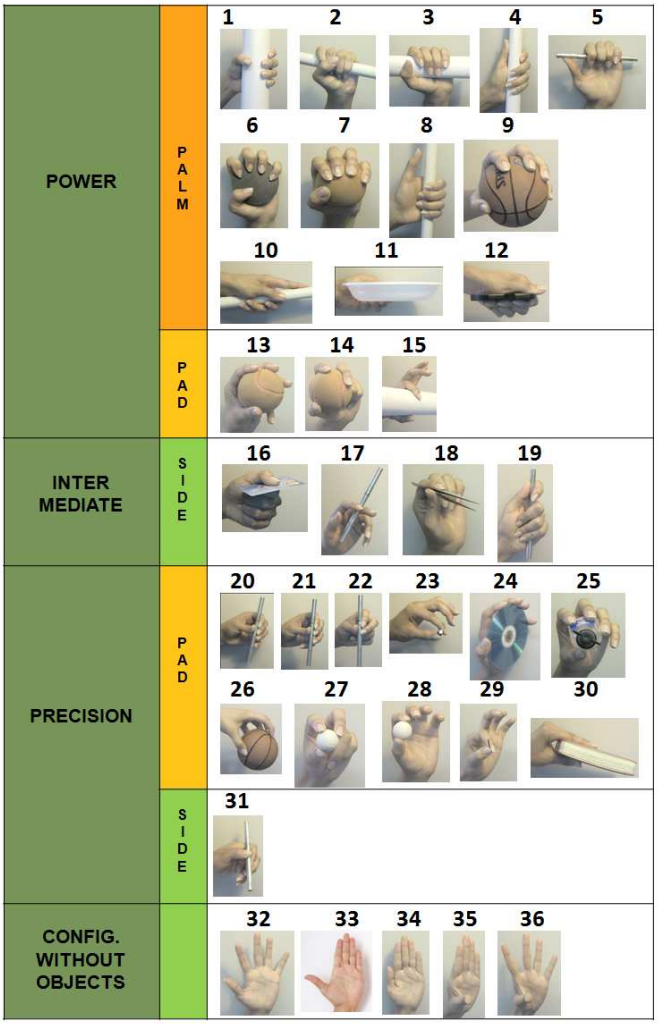

Figure 2: Reference set of comprehensive human grasps and open-hand configurations used for PCA [4].

computation because, due to its linearity, it allows planning the reach-to-grasp movements of the robot hand by means of a simple linear interpolation of the synergies. Moreover, PCA is faster than other methods, it allows finding global optima and it shows good performance in representing new grasps, as the experiments on new object/grasps pair synthesis reported in this paper demonstrate. Indeed, experimental results show that the grasp planning performed on the UB Hand IV by considering the three predominant pos-

tural synergies allows synthesizing and performing the whole reference set of grasps, which includes objects with different shapes and dimensions. The new contribution of this work with respect to the state of the art, reported in the next section, consists in the enrichment of the results obtained in previous works [4, 5, 6], by carrying out additional experiments in order to prove the efficiency of the synergy-based planning method in synthesizing new grasp/object pairs not contained in the reference set. Moreover, the general properties of the three predominant eigengrasps have been analyzed and compared with the ones of other two anthropomorphic robot hands.

The paper is organized as follows: Section 2 describes research work related to postural synergies. In Section 3 the UB Hand IV design characteristics are illustrated together with its kinematics and the one of the other two robotic hands used for comparing the results on postural synergies. Section 4 provides the description of the method adopted for deriving the hand postural synergies and some evaluations on the kinematic patterns of the three predominant eigenpostures. Moreover, the synergy-based planning method adopted for the experimental execution of the grasps is described. In Section 5 the use of the three predominant synergies for the grasp synthesis, the comparison with the case of two synergies only and the synthesis of new grasp/object pairs beyond the set of 36 hand configurations is shown through experimental results. Finally, Section 6 provides the conclusions and a sketch of future work.

2. Related Works

Recently, the studies of postural synergies have collected the interest of many researchers not only belonging to the field of neuroscience but also working on control theory and mechanical design of artificial hands.

In [1] the PCA has been used to calculate the postural synergies from real-world data collected on a variety of human hand postures by means of a data glove. Moreover, the authors show that a wide set of hand postures during grasping operation evolves continuously within a linear space spanned by two postural synergies that account for >80% of the hand configurations variance, without distinguishing between power and precision grasps. In [2] it is shown that even if higher principal components account for a small percentage of the variance, they give critical details not only for the static grasp when the hand adapts to the object shape, but also for the act of preshaping during the grasp. In [7] and [8] the authors extend the concept of postural synergies

to robotic hands showing how a similar dimensionality reduction can be used to derive comprehensive planning and control algorithms that produce stable grasps for a number of different robot hand models.

In [9] the configurations of the human hand are divided in 17 groups according to the different joints involved in each task, and the number of data samples per group is suitably selected to give to each group the same coverage according to the number of joints involved. The acquisition of the human hand motions is then carried out by means of a sensorized glove and the PCA is applied to the collected data to detect the principal motion directions, then the results are transferred to a robotic hand. In [10] a synergy-based impedance controller has been derived and implemented on the DLR hand. Mapping synergies from the human hand to the robot hand has been addressed in [11], where a strategy based on the use of a virtual sphere has been adopted for mapping the synergies between a paradigmatic human hand and a robotic hand in the task space. This approach has the advantages to be independent from the robotic hand, whereas it depends only on the specific operation, and thus it can be used for robotic hands with very dissimilar kinematics.

In [12] three synergies have been extracted from data on human grasping experiments and mapped to a robotic hand. Then a neural network has been trained with the features of the objects and the coefficients of the synergies and has been employed to control robot grasping. Neural networks have been utilized also in other works [13, 14] in order to simulate temporal coordination of human reaching and grasping. In [14] a neural network model for synergy-based control of the fingers motion during prehension is developed together with the design of a hand gestures library. This work shows how neural networks in combination with postural synergies allow to synthesize grasps on the basis of few parameters like object shape, dimension, position and orientation.

Several studies have also been carried out in order to simplify the design of robotic hands structure [15]. In [16] the authors investigate how the synergies number and type are related to the possibility of controlling the contact forces and the object motion in grasping and manipulation tasks. In [17], by using the definition of force closure for underactuated hands and the definition of grasping force optimization, the authors investigate how different postural synergies affect two case studies, i.e. a precision and a power grasp, considering the force closure and the grasp quality indexes. In [18] the manipulability analysis has been extended to synergy-actuated hands, where

the compliance is exploited in order to solve the force distribution problem. The authors introduce new manipulability indexes which take into account underactuation and compliance. In [19] the mechanical compliance of the hands musculotendinous system has been considered in the definition of the synergies in order to account for the force distribution in the actual grasp.

Besides the PCA, there are several non-linear methods for dimensionality reduction, such as Isomap, BP-Isomap and GPLVM that are discussed and compared with PCA in [20, 21]. In [21], the authors address the problem of noise in pose graph construction when noisy data-sets, such as motion capture, are used. They found that using extension to Isomap (BP-Isomap) instead of PCA improves the quality of the computed subspace. In [20] a Gaussian Process Latent Variable Models (GPLVMs) is used to model the lower dimensional manifold of human hand motions during object grasping. The authors demonstrate that this non-linear tool presents better performance in reconstructing spatial and temporal grasping actions with respect to both PCA, that is limited due to its linearity, and Isomap or LEE, that are very sensitive to noise since they are based on local distance measurements. In [22] a dimensionality reduction for manipulation tasks based on the Unsupervised Kernel Regression (UKR) method is applied to the problem of turning a bottle cap.

3. Description of the Robotic Hands Used for Synergies Evaluation

In this section, the devices considered in this paper for the evaluation of the postural synergies are briefly described. Particular emphasis is given to the UB Hand IV since it has been adopted also in the experiments hereby reported. The evaluation of the postural synergies has also been applied to other two robot hands with the aim of deriving common features that do not depend on the particular kinematics nor on the number of fingers.

It is worth noticing that, since the aim of this work is the reproduction of human-like grasping behavior, the analysis is restricted to anthropomorphic robotic hands with four or five fingers. A four-fingered hand represents an interesting case study since, from the point of view of the functionality, in many common grasps the ring and the little fingers act as a whole, hence this solution has been adopted for simplifying the design of many robotic hands [23]. On the other hand, the problem of converting a human-like grasp in a suitable grasp for robotic hands with non-anthropomorphic kinematics and/or with different number of fingers is out of the scope of this work.

3.1. The UB hand IV

In Fig. 1 the first prototype of the UB Hand IV [24, 25, 26] developed within the DEXMART project [27] is shown. This innovative anthropomorphic robot hand has been designed aiming at achieving human-like manipulation capabilities and mobility while pursuing the maximum design simplification and reduction of the device's cost production and development. To this end, the UB Hand IV has been conceived by taking into account the following driving issues.

i) The hand mechanics is based on an endoskeletal structure articulated by means of pin joints, integrated into the phalanx body, simply consisting in a plastic shaft which slides on a cylindrical surface [24, 28, 29].

ii) Remotely located actuators with tendon-based transmissions routed by sliding paths (*sliding tendons*) [30, 31, 32] have been adopted for the joints actuation.

iii) A purposely designed soft cover mimicking the human skin [33, 34, 35] has been introduced for improving the grasping capabilities of the hand.

iv) The mechanical structure of the hand has been manufactured adopting additive technologies like Fused Deposition Manufacturing or Stereo-Lithography.

Inspired also by the biological model, the actuators of the UB Hand IV have been placed in the forearm and tendons have been adopted for motion/force transmission from the forearm to the wrist and the fingers. Taking into consideration the general design objectives, an $N + 1$ tendon configuration has been adopted for reducing at minimum the number of actuators while preserving full motion capabilities and avoiding the use of pretension mechanisms. The reader is referred to [36] for a complete description of the UB Hand IV finger kinematics and tendon network characteristics. In order to reduce the complexity of the hand control, an internal unactuated (passive) tendon has been introduced to couple the movements of the last two joints of each finger, i.e. the medial and the distal joint, in such a way that $\theta_3 = \theta_4$. Hence, only three angles for each finger are considered, the base (adduction/abduction) angle θ_1, the proximal angle θ_2 and the medial angle θ_3. A total amount of $h = 15$ joint angles is then used for describing the robotic

hand configuration. The joint angles ranges of each finger are mechanically constrained by stroke limiters within the intervals:

$$\theta_1 \in [-10,\, 10], \quad \theta_{\{2,\,3,\,4\}} \in [0,\, 90] \quad [\text{deg}]. \tag{1}$$

For the sake of brevity and since the discussion of the UB Hand IV characteristics is not the main topic of this paper, only the Denavit-Hartenberg parameters of each finger are reported in Tab. 1.

Table 1: Denavit-Hartenberg parameters of the UB Hand IV fingers.

Link	d	θ	a [m]	α [deg]
1	0	θ_1	$a_1 = 20.2 \cdot 10^{-3}$	90
2	0	θ_2	$a_2 = 45.0 \cdot 10^{-3}$	0
3	0	θ_3	$a_3 = 29.9 \cdot 10^{-3}$	0
4	0	θ_4	$a_4 = 21.8 \cdot 10^{-3}$	0

3.2. Kinematics of the DEXMART Hand

On the basis of the experience gained from the UB Hand IV and with the purpose of moving closer to the human manipulation capabilities and mobility, a new kinematics has been designed for the development of a new five-fingered hand prototype, namely the DEXMART Hand. In the new design, the main changes are related to the differentiation of the dimensions of each finger, to the joint limits and to the kinematics of the thumb. In particular, the adduction/abduction base joint and the first flexion joint of the thumb have been inverted in the kinematic chain. The main objective in the design of the new hand kinematics is to achieve the opposition of the thumb with the other fingers. The Denavit-Hartenberg parameters reported in Tab. 2 are different for all the fingers in order to have a better fitting with the human hand kinematics. The joint angles needed to describe the hand configuration are the same of the UB Hand IV, then a total amount of $h = 15$ joint angles describes the robotic hand configuration also in this case. Denoting with the subscripts t and f the joint of the thumb and of the other finger respectively, the joint angles ranges for each finger are mechanically constrained by stroke limiters within the intervals:

$$\theta_{1f} \in [-10,\, 10], \quad \theta_{2f} \in [0,\, 90], \quad \theta_{3f} \in [0,\, 110] \quad [\text{deg}] \tag{2}$$

$$\theta_{1t} \in [0,\, 90], \quad \theta_{2t} \in [0,\, 60], \quad \theta_{3t} \in [0,\, 90] \quad [\text{deg}]. \tag{3}$$

The analysis of the postural synergies of the hand kinematics described above, other than being useful for deriving characteristics of the synergies that are independent from the particular kinematics, allows gaining information about the properties of this kinematics before the production of the robot hand prototype.

Table 2: Denavit-Hartenberg parameters of the DEXMART Hand.

Link (Thumb)	d [mm]	θ	a [mm]	α [deg]
1	-42.5	$\theta_1 + 85$	18	-90
2	-1.65	$\theta_2 - 80$	24.57	70.32
3	4.89	$\theta_3 + 10.62$	30	0
4	0	$\theta_4 - 3.61$	30	0
Link (Index)	d [mm]	θ	a [mm]	α [deg]
1	-2.91	θ_1	18	90
2	0	$\theta_2 - 20$	38	0
3	0	θ_3	28	0
4	0	θ_4	28.5	0
Link (middle)	d [mm]	θ	a [mm]	α [deg]
1	-4.91	θ_1	18	90
2	0	θ_2	40	0
3	0	θ_3	28	0
4	0	θ_4	28.5	0
Link (Ring)	d [mm]	θ	a [mm]	α [deg]
1	-1.93	θ_1	18	90
2	0	$\theta_2 - 5$	38	0
3	0	θ_3	28	0
4	0	θ_4	28.5	0
Link (Little)	d[mm]	θ	a [mm]	α [deg]
1	4.24	θ_1	18	90
2	0	$\theta_2 + 15$	35	0
3	0	θ_3	28	0
4	0	θ_4	28.5	0

3.3. A Four-Fingered Anthropomorphic Robot Hand

The ability of some prototypes of anthropomorphic robot hands with four fingers only, such as the DLR/HIT hand [23], in executing human like

grasping and manipulation tasks is reported in literature [10]. Aiming at the investigation of common features of postural synergies, also the number of fingers should be considered as a parameter. For this reason, the postural synergies have been evaluated on a robot hand with the same kinematics of the UB Hand IV, whose Denavit-Hartenberg parameters are reported in Tab. 1 but with four fingers only (the little finger has been removed), obtaining a kinematic configuration similar to the one of the DLR/HIT hand. A total amount of $h = 12$ joint angles are necessary in this case to describe the robot hand configuration.

4. Postural Synergies of the UB Hand IV

Drawing inspiration from the studies on the human hand motion [1], and since the UB Hand IV presents human-like kinematics, a set of postural synergies of the UB Hand IV configuration space has been found. The details of this analysis are reported in the following.

4.1. PCA Analysis

The UB Hand IV kinematics is rather close to that of the human hand. Hence, with the aim of deriving the PCA, a set of grasps similar to those illustrated in [3] hand has been considered. The choice of the reference set of postures, reported in Fig. 2, has been made by taking into account all the most common human grasps considered in the grasp taxonomy literature. Only two of the configuration reference set shown in [3] were not considered in this work due to limitations in the kinematics of the robotic hand with respect to the capabilities of the human one. A total amount of $n = 36$ hand configurations has been evaluated to derive the fundamental eigenpostures. Three main groups of hand configurations have been considered, such as precision, intermediate and power grasps. For what concerns power grasps, this set considers both palm and pad grasps (depending on whether or not the grasp involve the entire palm) of circular objects, such as spheres and disks, and cylindrical objects of different dimensions, distinguishing also between different positions of the thumb. Moreover, several configurations for precision grasps with opposition of the thumb to the index only or to more than one finger (forming a virtual finger) are considered. Among precision grasps, configurations that involve both the pad and the side of the fingers have been considered. Finally, intermediate side grasps have been included. By observing the human hand motion, a subset of hand joints (adduction/abduction

and proximal joints of both fingers and thumb) whose limit positions are not reached in the selected grasp configurations have been identified. Since our aim is to define a set of synergies that can be used also for controlling the hand during the reach-to-grasp phase, a complete coverage of the hand movements in the reduced configuration subspace is necessary. Thus, a fourth group of open hand configurations has been added. This fourth group is obtained by considering different combinations of the adduction/abduction finger and thumb joints. Obviously, the selection of the grasps appearing in the reference set is based on a suitable trade-off between the coverage of the whole grasp taxonomy [3], the required time and complexity of the experimental evaluation, that increases with the number of reference postures, and the usage of synergies not only for grasps synthesis but also for controlling the hand during the reach-to-grasp phase.

Each configuration of the reference set of postures has been experimentally reproduced with the UB Hand IV as close as possible to a natural human-like grasp (as shown in Fig. 2) by moving the fingers, via the user software interface based on MATLAB/Simulink, until the contact with the object is reached. When the desired configuration is obtained and the overall grasp is stable, the vector $\mathbf{c}_i \in \mathbb{R}^{15}$ of the joint angle values corresponding to the reproduced grasp is measured. A weak point in this procedure is that the quality of both the finger contact on the object surface and of the overall grasp configuration with respect to the reference one relies on the evaluation of the human operator that moves the robotic hand. To solve this issue, contact detection algorithms [37] or force and tactile sensors [38, 39, 40] and camera-based posture evaluation will be introduced in future activities.

Once the matrix $\mathbf{C} = \{\mathbf{c}_i, \ldots, \mathbf{c}_n\}$ containing the entire set of the UB Hand IV configurations has been built, the vector $\bar{\mathbf{c}}$ representing the mean hand position in the grasp configurations space (zero-offset position) and the matrix $\mathbf{F} = \{\mathbf{c}_i - \bar{\mathbf{c}}, \ldots, \mathbf{c}_n - \bar{\mathbf{c}}\}$ of the grasp offsets with respect to the mean configuration have been computed. The PCA has then been performed on $\mathbf{F}$ and a base matrix $\mathbf{E}$ of the postural synergies subspace has been found. The PCA can be performed by diagonalizing the covariance matrix of $\mathbf{F}$ as

$$\mathbf{F}\,\mathbf{F}^T = \mathbf{E}\,\mathbf{S}^2\,\mathbf{E}^T. \tag{4}$$

The $(h \times h)$ orthogonal matrix $\mathbf{E}$ gives the directions of variance of the data, where $h = 15$ gives the size of the whole configuration space of the hand. The diagonal matrix $\mathbf{S}^2$ is the variance in each direction sorted in decreasing

magnitude, i.e. the element on the diagonal represents the eigenvalue of the covariance matrix.

To verify the effectiveness of the synergy-based modeling approach, the percentage σ of the total variance of the data described by the first j-th principal components can be obtained by means of the following equation

$$\sigma_j = \sum_{k=0}^{j} \mathbf{s}_k \Big/ \sum_{k=0}^{15} \mathbf{s}_k \tag{5}$$

where $\mathbf{s}_k$ is the k-th element of the diagonal of the matrix $\mathbf{S}^2$. The first two synergies found for the UB Hand VI account for >77% of the hand postures, thus matching quite well the results reported in [1]. Since the three principal components account for >85% of the postures ($\sigma_3 = 0.8503$), the posture matrix $\mathbf{C}$ can be reconstructed with good accuracy by adopting the matrix

$$\hat{\mathbf{E}} = [\mathbf{e}_1 \ \mathbf{e}_2 \ \mathbf{e}_3] \tag{6}$$

composed of the three principal components of $\mathbf{E}$ as a base of the robotic hand configuration space, thus allowing the control of the robotic hand motion in a configuration space of highly reduced dimensions with respect to the DoFs of the hand itself. Each hand grasp posture $\mathbf{c}_i$ can be obtained by a suitable selection of the coefficients $[\alpha_1 \ \alpha_2 \ \alpha_3]^T \in \mathbb{R}^3$ of the postural synergies. Therefore, the projection $\hat{\mathbf{c}}_i$ of each robotic hand configuration $\mathbf{c}_i$ on the postural synergies subspace can be evaluated as

$$\hat{\mathbf{c}}_i = \bar{\mathbf{c}} + \hat{\mathbf{E}} \begin{bmatrix} \alpha_{1,i} \\ \alpha_{2,i} \\ \alpha_{3,i} \end{bmatrix}. \tag{7}$$

In the following, the three fundamental synergies derived for the UB Hand IV, i.e. the robotic hand motions spanned by $\mathbf{e}_1$, $\mathbf{e}_2$ and $\mathbf{e}_3$ respectively, are briefly described, referring to the minimum and maximum configuration of each synergy as the hand configurations obtained by means of, respectively, the minimum and maximum value of the corresponding synergy coefficients without violating the joint limits (1). When the coefficients of the synergies are zero, the hand posture corresponds to the zero-offset position $\bar{\mathbf{c}}$. The circular graphs represented in Fig. 3(a) are a useful tool for identifying the joints whose rotations are more involved in each synergy. From left to right, the angular variations in degrees for each joint due to a unitary variation of

the corresponding synergy coefficient is represented for the first, the second and the third synergy. It is easy to observe how the adduction/abduction thumb joint motion (joint #1) is more involved in the third synergy rather than in the first two. Moreover, in the third synergy the movement of the index and of the thumb are more engaged than for the other fingers. This justifies the use of the third synergy in order to grasp objects more precisely, especially for precision grasps and intermediate side grasps, where the position of the thumb and of the index is crucial, as the experiments reported in Section 5 demonstrate.

4.2. Synergy Patterns Description

With reference to the first postural synergy, in the minimum configuration the proximal and medial flexion joint angles of all the fingers are all almost zero and increase their value during the motion toward the maximum configuration (this feature is also present in the human hand first synergy [1]). The adduction/abduction movements are not very involved in this synergy. In Fig. 4(a) the minimum, zero-offset and maximum configuration in frontal and lateral view of the UB Hand IV first postural synergy are represented.

The second postural synergy is characterized by a movement in opposite directions of the proximal and medial flexion joints (this feature is also present also in the human hand second synergy [1]). In this synergy, the adduction/abduction movements of all the fingers are more involved with respect to the first synergy for the index and the little finger. In Fig. 4(b) the minimum, zero-offset and maximum configurations of the UB Hand IV second postural synergy are depicted in frontal and lateral views.

In the third postural synergy, the movement of the index and the thumb are mainly involved.

Thanks to this synergy, the movement of adduction/abduction of the thumb covers the whole joint range without violating other joint limits. This characteristic is crucial because the correct index/thumb opposition allows increasing the grasp accuracy, and thus achieving more stable grasps as will be discussed in detail in the following. This justifies the use of three predominant synergies for the hand control in order to improve the grasp performance. Finally, the variation of the adduction/abduction angle of the middle and ring fingers is larger in this synergy rather than in the first two. In Fig. 4(c) the minimum, zero-offset and maximum configuration in frontal and lateral views of the UB Hand IV third postural synergy are represented.

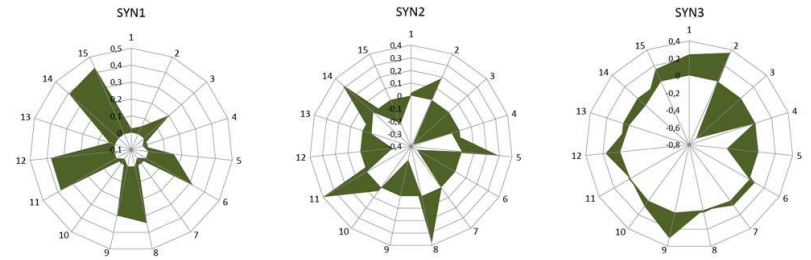

(a) UB Hand IV [4].

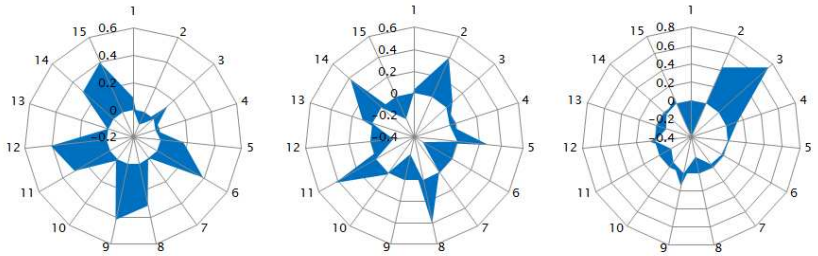

(b) DEXMART Hand.

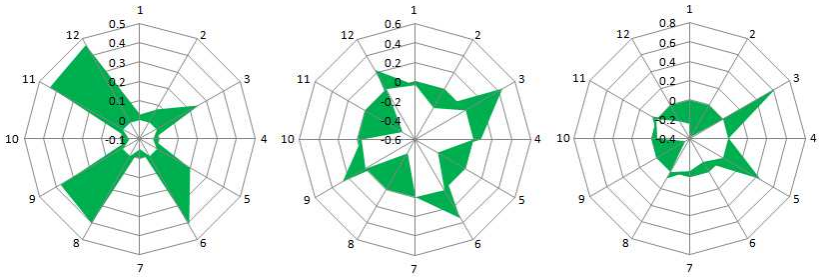

(c) Four fingered anthropomorphic hand.

Figure 3: In these figures, the angular change in degrees for each joint due to a positive unitary variation in α_1, α_2, and α_3 for the first three synergies are represented. The adduction/abduction, proximal and medial flexion joints are indicated from 1 to 3 for the thumb, from 4 to 6 for the index finger, from 7 to 9 for the middle finger, from 10 to 12 for the ring finger and finally from 13 to 15 for the little finger.

4.3. Kinematic Comparison with Different Hand Prototypes

In order to derive common features, the three predominant synergies for the other two robot hands described in Sect. 3.2 and 3.3 respectively have been computed using the same method and the same data-set adopted for the UB Hand IV. The postural synergies of those anthropomorphic hands have

been compared to the ones of the UB Hand IV using the circular graphs reported in the Fig. 3(a), 3(b) and 3(c). From these figures, it is possible to note that the main features of the three predominant synergies discussed in Sect. 4.2 are preserved also in the case of a different kinematics, see Fig. 3(b), or in the case of a different number of fingers, see Fig. 3(c). In particular, Fig. 3 shows that the motion of the thumb adduction/abduction angle (index 1 in the circular graphs) is mainly involved in the third synergy rather than in the other two, even if the sign of the thumb adduction/abduction activation is changed in Fig. 3(b) and 3(c) with respect to Fig. 3(a).

4.4. Planning Reach to Grasp Movements with Postural Synergies

In order to perform the i-th grasp, the three predominant synergies, whose motion patterns are described in Sect. 4.2 and Fig. 4, are linearly combined. The values of the three synergy coefficients $[\alpha_1 \ \alpha_2 \ \alpha_3]^T$ appearing in (7) are computed by projecting the desired configuration $\mathbf{c_i}$ (the i-th grasp posture of the matrix $\mathbf{C}$) in the synergy subspace, i.e.

$$\begin{bmatrix} \alpha_{1,i} \\ \alpha_{2,i} \\ \alpha_{3,i} \end{bmatrix} = \hat{\mathbf{E}}^{\dagger} \left(\mathbf{c}_i - \bar{\mathbf{c}} \right) \tag{8}$$

where $\hat{\mathbf{E}}^{\dagger}$ is the Moore-Penrose pseudo-inverse of the base matrix $\hat{\mathbf{E}}$. It is straightforward to note that the motions shown in Fig. 4(a), 4(b) and 4(c), derived by considering separately the three synergies, are obtained from (7) by assuming $\alpha_2 = 0$ and $\alpha_3 = 0$ for the first synergy, $\alpha_1 = 0$ and $\alpha_3 = 0$ for the second synergy, and finally $\alpha_1 = 0$ and $\alpha_2 = 0$ for the third synergy. The video footage to this paper shows the pattern's motion of each synergy and the results of the grasp experiments. The value of the coefficients α_1, α_2, α_3 changes in time during the grasp execution in such a way that, starting from the zero-offset position $\bar{\mathbf{c}}$ (i.e. $\alpha_1 = \alpha_2 = \alpha_3 = 0$), the hand opens, during the reach phase, and then closes achieving a suitable shape determined by means of (8) and depending on the original grasp configuration $\mathbf{c}_i$ for the considered object. In the open-hand configuration, namely $\mathbf{c}_0$ (corresponding to $\mathbf{C}_{32}$ in Fig. 2), all the flexion joint angles are close to zero, and the corresponding values of α_1, α_2 and α_3 can be determined from (8). The planned open hand configuration is the same for all the objects, and thus it is chosen independently of the object shape. The values of the synergy coefficients during the grasp execution are computed through linear interpolation of the

α_1, α_2 and α_3 values in the three reference configurations $\{\bar{\mathbf{c}},\ \hat{\mathbf{c}}_0,\ \hat{\mathbf{c}}_i\}$ by assuming a suitable time interval, three seconds for both the opening and closing phases, for the grasp execution.

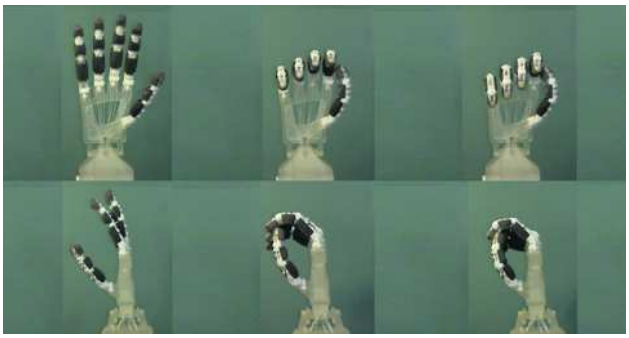

(a) First postural synergy.

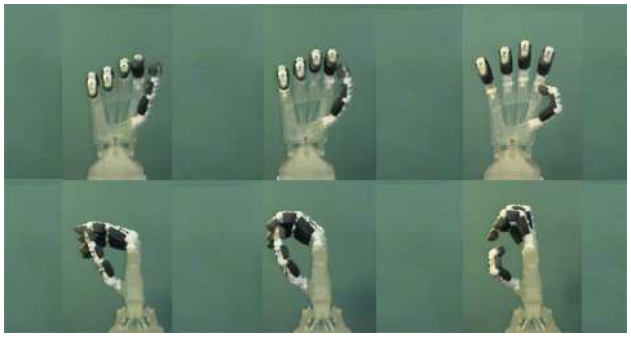

(b) Second postural synergy.

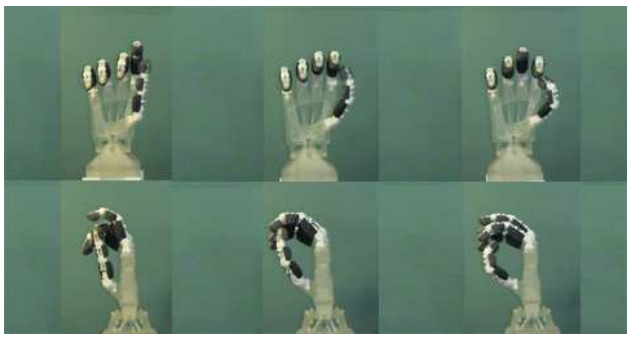

(c) Third postural synergy.

Figure 4: Representation of the UB Hand IV postural synergies. On the top of each figure, from left to right, a sequence of hand postures going from the minimum to the maximum configuration are represented. On the bottom the lateral views are reported.[4]

4.5. Evaluation of the Grasps Quality

In [17], using the definition of force-closure for underactuated hands and the definition of grasping force optimization, the authors demonstrate that the first two synergies are sufficient to establish force-closure. The results obviously depend on the location of the contact points on the object. Nevertheless, the third synergy gives an important rate on the improvement of the quality, as it is possible to observe in [17]. This is even more remarkable considering that, by investigating the role of different postural synergies in the quality of the grasps, no improvement has been observed beyond the first three synergies in the precision grasp case, while continuous but small improvements are observed in the power grasp case. Aiming at a quantitative evaluation of the improvements given by the introduction of the third synergy, the quality of the grasps has been evaluated for some configurations contained in the data-set. For this purpose, the free MATLAB toolbox SynGrasp [41] has been used. In particular, two precision grasps, C25 and C26 (which are reported in Fig. 7), that are successfully executed during the experiments by using three synergies (with respect to the case of two synergies only [5, 6]), have been considered as case studies to show the benefit that the third synergy gives in the positioning of the thumb. The internal contact forces are exerted along the line passing through the virtual finger (V.F. in Fig. 7, i.e. the centroid of the four fingertips opposed to the thumb) and the thumb. Thus, a possible measurement of the grasp quality can be given by the distance between this line and the center of mass of the object (O.C. in Fig. 7) [42]. By observing Fig. 5 it is possible to note that this distance is smaller for Configuration C26 in the bottom obtained using three synergies. The measures for two configurations that consider four and five fingers in contact are reported. For Configuration C26 the measures corresponding to the use of the first two and the first three synergies are 45.1 [mm] and 36.8 [mm] respectively, for Configuration C25 (four fingers in contact) they are 23.4 [mm] and 17.5 [mm] respectively. Considering the whole configuration subspace (15 synergies) the quality measures for Configurations C25 and C26 are 12.7 and 35.8 [mm] respectively. In order to verify similarities on the role of the third synergy among different kinematics, these quantitative measurements have been evaluated on the DEXMART Hand due to the correspondence with the UB Hand IV regarding the number of fingers involved in the considered configurations. The results are reported in Tab. 3. Thus, in both the kinematics it is observed that by adding the third synergy, a relevant improvement in the grasp quality is achieved with respect to the

Table 3: Grasp Quality Measures In Configurations C25 and C26.

	UB Hand IV	DEXMART Hand
C25 (two syn)	23.4 [mm]	20.0 [mm]
C25 (three syn)	17.5 [mm]	12.6 [mm]
C26 (two syn)	45.1 [mm]	54.1 [mm]
C26 (three syn)	36.8 [mm]	45.4 [mm]

case of two synergies only. These analytical results justify what comes out from our experiments, i.e. the grasp in which the opposition of the thumb with the other fingers is crucial to hold the object cannot be approximated precisely enough using two synergies only, that translates in unstable grasps during the experiments. This is especially true for precision grasps.

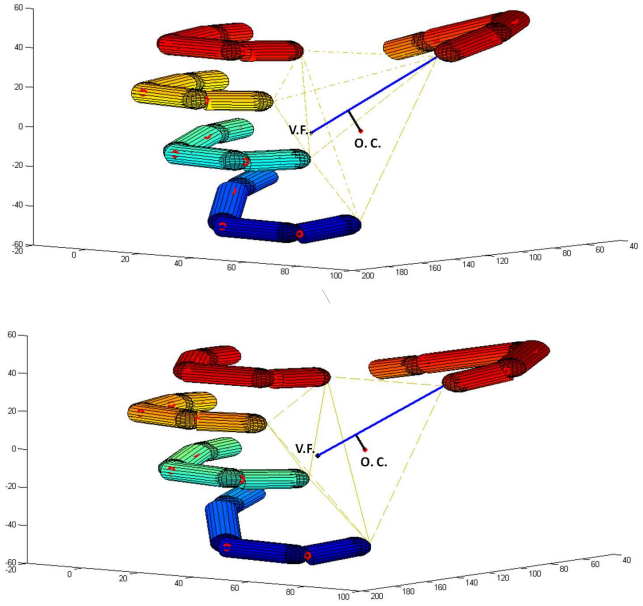

Figure 5: On the top, the UB Hand IV in Configuration C26, approximated using two synergies, is represented; on the bottom the same configuration is obtained using three synergies.

5. Experimental Evaluation of the Synergy-Based Grasp Synthesis

The hand controller developed in the MATLAB/Simulink environment is based on the RTAI-Linux realtime operating system. The MATLAB Real-time Workshop toolbox has been used for the automatic generation of the real-time application of the UB Hand IV controller. The user interface to the real-time application has been implemented by means of the Simulink External Mode capabilities, for which the RTAI-Linux support has been purposely developed. In the experiments, starting from the zero-offset position, the hand moves continuously in the synergies configuration subspace and goes in an open-hand configuration. Then, it closes reaching a configuration that depends on the particular grasp to be performed. During the closing phase, the coefficients of the three postural synergies are obtained by linear interpolation from those corresponding to the open-hand configuration to those suitable values unique for each object and computed using (8). It is important to remark that, besides the grasp planning simplification given by the proposed synergy-based method, the grasps synthesized by means of synergies are effectively executed even without a precise positioning of the object with respect to the hand, as shown in the attached video. Indeed, during grasp execution the human operator just approximatively places the object inside the hand in the expected object position for the reference grasp. Moreover, since the UB Hand IV is not equipped with tactile sensors, the contact with the object cannot be detected, however the grasp can be properly executed. A key role in achieving this result is played by the intrinsic compliance of the UB Hand IV transmission system and mechanical structure, that allows a certain adaptation of the hand to the grasped object even in case of both limited precision in the hand configuration, due to the synergy-based planning, and uncertainties in the object shape, dimension and position with respect to the hand. Experimental results reveal that, by using the three predominant eigengrasps, it is possible to reproduce several grasp configurations more precisely than in the case of using two synergies only [5], see Figs. 6, 7 and 8. In particular, by adding the third synergy, configurations C18, C19, C25, C26 and C28 have been executed in a stable and repeatable way, whereas in [5] these grasps have not been successfully performed using two synergies only. The evaluations of the experimental data have been carried out with the aid of bar plot and graphs. Figure 9 reports the bar plot of the coefficients of the first three synergies obtained by projecting the 36 postures in the three predominant synergies subspace. In Fig. 10 the angle error (in absolute value)

Figure 6: Reproduced power grasps from the reference set of postures using the first three synergies [4].

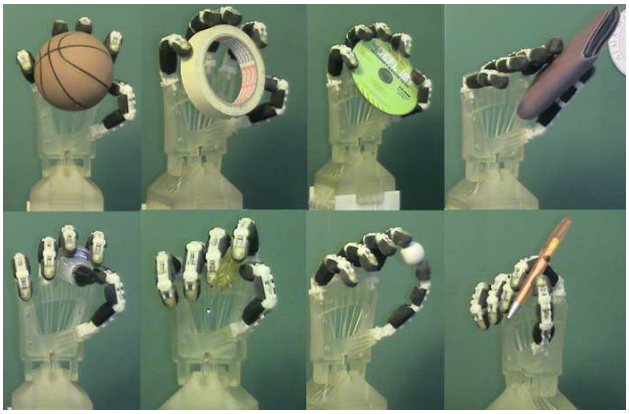

Figure 7: Reproduced precision grasps from the reference set of postures using the first three synergies [4].

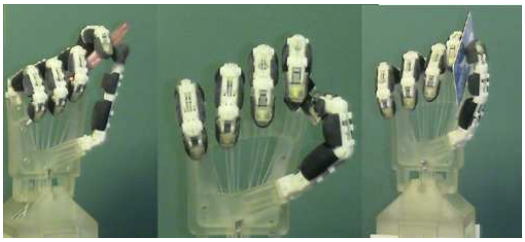

Figure 8: Reproduced intermediate side grasps from the reference set of postures using the first three synergies [4].

of the adduction/abduction joint of the thumb obtained comparing the configurations of the reference set with the reproduced configurations using two and three synergies are graphically reported. Finally, the average value of the joint errors in the case of using two and three synergies are reported in Fig. 11, where it is also possible to appreciate the improvement obtained by the introduction of the third synergy. The average of value the joint errors is

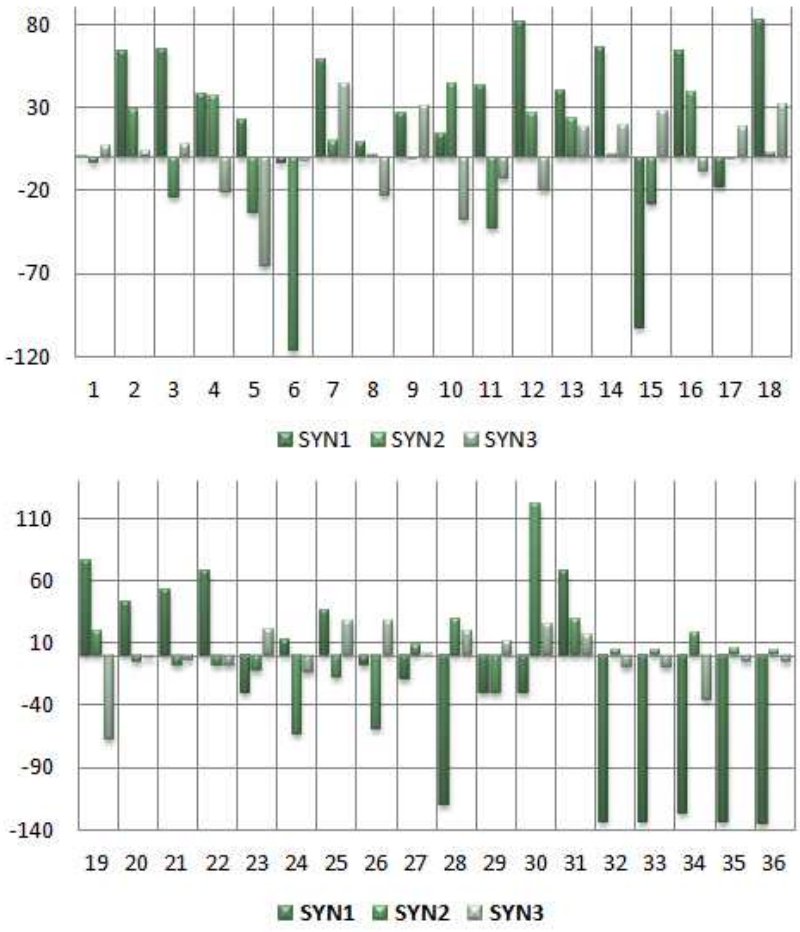

Figure 9: The bar plot represents the coefficients of the first three synergies for each of the reference configuration (Fig. 2) projected in the 3D latent subspace.

computed using the Euclidean norm $e = \frac{\|\mathbf{c_i} - \widehat{\mathbf{c}}_\mathbf{i}\|}{15}$. By observing the first image from the left (pen, Configuration C19 in Fig. 9) of Fig. 8, it is interesting to note that this posture is very close to the minimum configuration of the third synergy; indeed the coefficient of the third synergy is high with respect to the other grasps, and thus the use of the third synergy is essential for this performance. Also the average value of the joint errors decreases significantly compared to the other grasps (see Fig. 11). By looking at Fig. 10 it is possible to note that the use of the three predominant synergies reduces

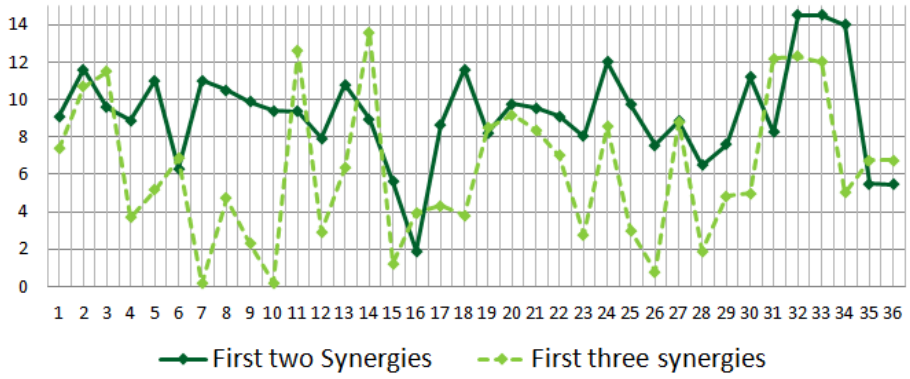

Figure 10: The angle error (in absolute value) of the adduction/abduction joint of the thumb obtained comparing the reference set of configurations and the reproduced configurations using two (continuous line) and three synergies (dashed line) is represented.

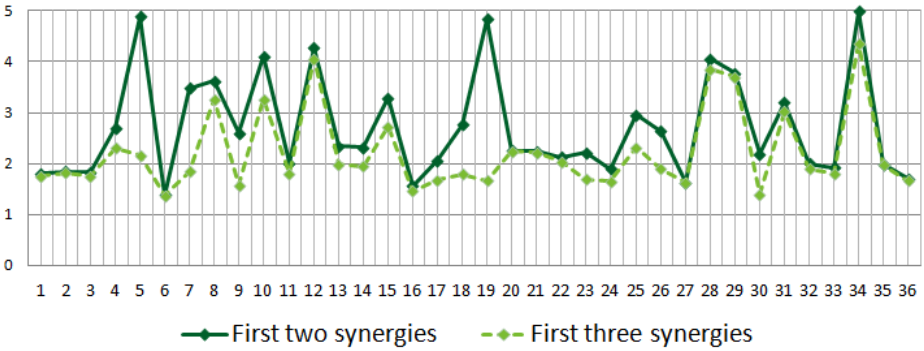

Figure 11: The average of the joint errors in the case of two (continuous line) and three synergies (dashed line) are reported.

the angular position error of the adduction/abduction joint of the thumb for 27 configurations over the 36 in the reference set with respect to the case in which only two synergies are considered. In Fig. 12 two grasp configurations executed using both two and three synergies are represented. From left to right by looking the first pictures of the ball and of the CD, that are the ones executed using three synergies, the improvement on the position of the thumb can be noticed. Only for Configuration C27 no improvement has been obtained and this is confirmed by the very small value of the third synergy coefficient and the joint errors (Fig. 10 and Fig. 11); this means that the third

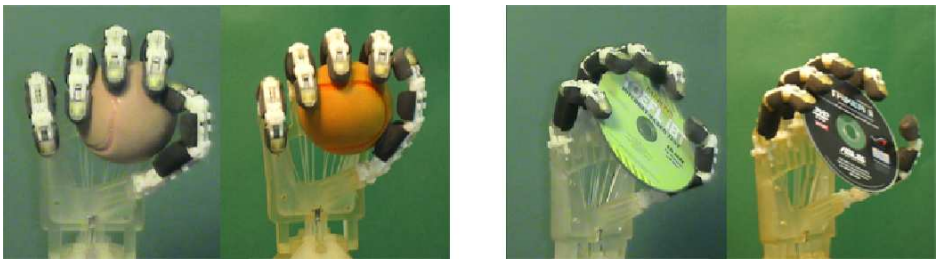

Figure 12: Comparison between two grasps configuration executed using both two and three synergies. From left to right the first pictures of the ball and of the CD are the grasps executed using three synergies.

synergy gives almost no contribution to this posture. The improvement on the adduction/abduction thumb joint angle using the third synergy is very clear at least for Configurations C18, C25, C26 and C28. For what concerns Configuration C19 (pen, intermediate side grasp), the improvement can be seen mainly in the error average. The implemented grasps show that through the use of the three predominant synergies the matrix of the reference set $\mathbf{C}$ (Fig. 2) can be reproduced with an accuracy greater than >85%. The idea now is to prove the ability of the method in generalizing grasps synthesis in the subspace of the three predominant postural synergies. To accomplish this goal, five grasps of common objects not contained in the reference set have been selected, see Fig. 13(a). The object/grasp pairs have been chosen so as to cover the entire variety of grasps taxonomy [3], with reference to Fig. 13(a), from left to right, namely a power palm grasp, a power pad grasp, an intermediate side grasp, a precision pad grasp, and a precision side grasp. The synthesis of these grasps using the whole hand configuration space involves complex problems of planning and control due to the high number of DoFs and complex anthropomorphic kinematics that are essential for these specific tasks. By adopting the same method used to define the configuration matrix $\mathbf{C}$, the robotic hand has been manually positioned in the desired grasp configuration and the joint displacement vector has been recorded. Through the projection of the measured configuration in the synergies subspace, the synergies coefficients in the final configuration $\hat{\mathbf{c}}_i$ have been evaluated. The coefficients are then used by the controller that performs the motion during reach-to-grasp, and the final grasp configurations are reported in Fig. 13(b). In Fig. 13(b), the position of the synergy coefficients corresponding to the final grasp configurations for all the objects successfully grasped during the

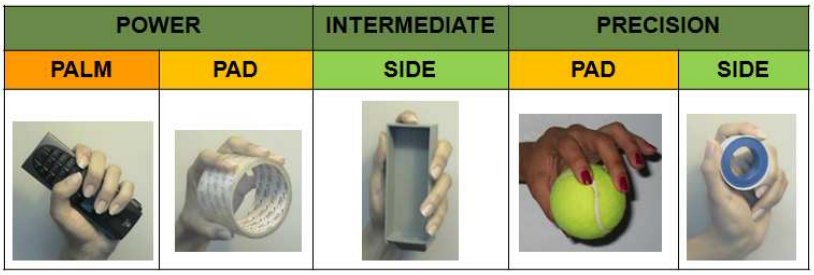

(a) Human hand grasps selected for synergy-based synthesis.

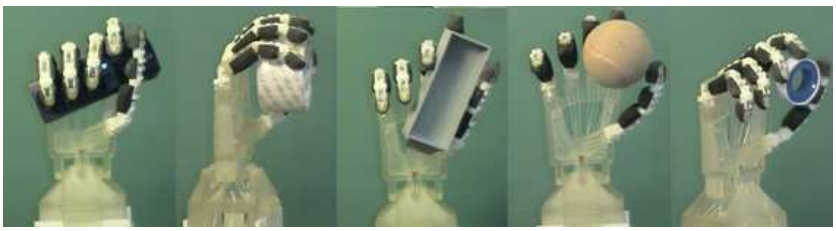

(b) Synthesized grasps with the UB Hand IV.

Figure 13: On the top, the reference set of human grasps not included in the PCA analysis is depicted. On the bottom, the synthesized grasps are realized with the UB Hand IV using synergies subspace projection is shown.

experiments is shown in the space of the three predominant synergies. In the figure 14, the synergy coefficients corresponding to the synthesized grasps obtained by projection in the synergies subspace of the desired configuration of the hand are indicated by a different marker (triangle). Further, an example of a complete hand trajectory computed by linear interpolation of the synergies coefficients in the three reference configurations for the grasp of a generic object (a CD) is reported using a red line.

6. Conclusions and Future Work

In this paper the experimental evaluation of the three predominant postural synergies of the UB Hand IV by means of PCA has been presented. For this purpose, a suitable reference set of hand postures has been taken into account. The kinematic patterns of the three predominant postural synergies have been described and the benefit given by the introduction of the third synergy, added to improve over a previous work, has been enlightened. Moreover, the introduction of the third synergy has been discussed from the

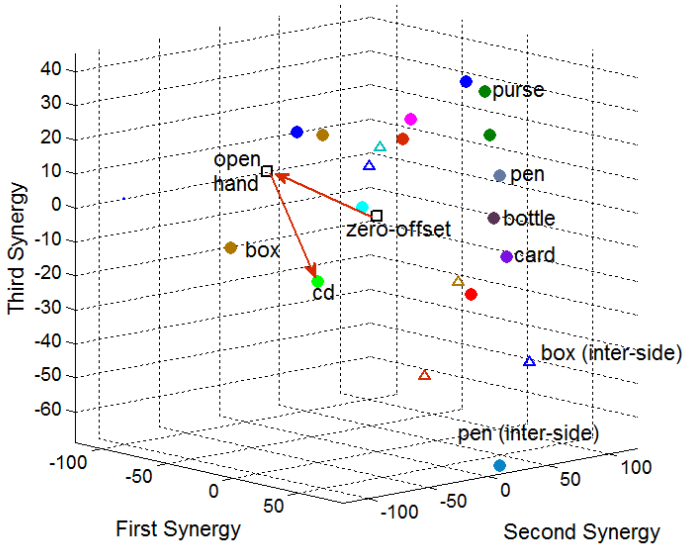

Figure 14: The distribution of hand postures, corresponding to the grasps executed during the experiments, is represented in the space of the first three postural synergies. The synthesized grasps not contained in the reference set of 36 postures are represented with a different marker (triangle).

point of view of the grasp quality in some significant and critical cases. An experimental activity has been performed for the evaluation of the synergy-based planning approach, and the results reported in this paper confirm that the proposed method can work efficiently for every considered object/grasp pair throughout a complete taxonomy. As a step forward the previous works available in literature, the synthesis of additional grasp/object pairs not included in the reference set of hand configurations and covering the whole grasp taxonomy has been successfully achieved. Moreover, the properties of the three predominant eigengrasps have been compared with the results obtained considering different anthropomorphic hand kinematics and the same grasps reference set. Since the main features of the first three synergies are preserved, and considering that the fundamental characteristics of the first two synergies of the UB Hand IV are similar to the human hand ones [1], we can conclude that the reference set of hand configurations for PCA is appropriate for transferring human hand grasp capabilities (synergies) to anthropomorphic robotic hands. Future work aims at deriving synergies on the basis of a larger data set including information from force/tactile sensors.

Moreover, to overcome the limits of the adopted grasp synthesis method, based on the knowledge of the desired grasp in the configuration space of complete dimension, a synergy-based planning strategy driven by a limited set of parameters, describing the object shape, dimension and position, will be investigated. Non-linear methods for dimensionality reduction will be also considered. Force closure tests will be used to determine the quality of the grasps and to properly choose the optimal coefficient of the synergies for grasp and manipulation tasks. The postural synergies evaluation will be also used to improve the kinematics of the UB Hand IV toward an increasing level of anthropomorphism.

Acknowledgments

The authors want to thank all those who have contributed in the recent years to the development of the UB Hand IV prototype. Further, the support of Umberto Scarcia and Ugo Fabrizi during the experiments described in this paper is gratefully acknowledged.

References

[1] M. Santello, M. Flanders, J. Soechting, Postural hand synergies for tool use, Journal of Neuroscience 18 (23) (1998) 10105–10115.

[2] C. Mason, J. Gomez, T. Ebner, Hand synergies during reach-to-grasp, Journal of Neurophysiology 86 (6) (2001) 2896–2910.

[3] T. Feix, R. Pawlik, H. Schmiedmayer, J. Romero, D. Kragic, The generation of a comprehensive grasp taxonomy, in: Robotics, Science and Systems, Workshop on Understanding the Human Hand for Advancing Robotic Manipulation, Washington, 2009.

[4] F. Ficuciello, G. Palli, C. Melchiorri, B. Siciliano, Planning and control during reach to grasp using the three predominant UB Hand IV postural synergies, in: Proc. IEEE Int. Conf. on Robotics and Automation, Saint Paul, 2012, pp. 2255–2260.

[5] F. Ficuciello, G. Palli, C. Melchiorri, B. Siciliano, Experimental evaluation of postural synergies during reach to grasp with the UB Hand IV, in: Proc. IEEE/RSJ Int. Conf. on Intelligent Robots and Systems, San Francisco, 2011, pp. 1775–1780.

[6] L. Villani, V. Lippiello, F. Ruggiero, F. Ficuciello, B. Siciliano, G. Palli, Grasping and control of multifingered hands, in: Advanced Bimanual Manipulation, B. Siciliano (Ed.), Springer Tracts in Advanced Robotics, vol. 80, Springer, 2012, pp. 219–266.

[7] M. Ciocarlie, C. Goldfeder, P. Allen, Dimensionality reduction for hand-independent dexterous robotic grasping, in: Proc. IEEE/RSJ Int. Conf. on Intelligent Robots and Systems, San Diego, 2007, pp. 3270–3275.

[8] M. Ciocarlie, P. Allen, Hand posture subspaces for dexterous robotic grasping, International Journal of Robotics Research 28 (7) (2009) 851–867.

[9] S. Sun, C. Rosales, R. Suarez, Study of coordinated motions of the human hand for robotic applications, in: Proc. IEEE Int. Conf. on Robotics and Automation, Anchorage, Alaska, 2010, pp. 776–781.

[10] T. Wimboeck, B. Jan, G. Hirzinger, Synergy-level impedance control for a multifingered hand, in: Proc. IEEE Int. Conf. on Intelligent Robots and Systems, San Francisco, 2011, pp. 973–979.

[11] G. Gioioso, G. Salvietti, M. Malvezzi, P. Prattichizzo, Mapping synergies from human to robotic hands with dissimilar kinematics: An object based approach, in: Int. IEEE Conf. on Robotics and Automation, Workshop on Manipulation Under Uncertainty, Shangai, 2011.

[12] T. Geng, M. Lee, M. Hulse, Transferring human grasping synergies to a robot, Mechatronics 21 (1) (2011) 272–284.

[13] A. Ulloa, D. Bullock, A neural network simulating human reachgrasp coordination by continuous updating of vector positioning commands, Neural Networks 16 (2003) 1141–1160.

[14] J. Vilaplana, J. Coronado, A neural network model for coordination of hand gesture during reach to grasp, Neural Networks 19 (1) (2006) 12–30.

[15] C. Brown, H. Asada, Inter-finger coordination and postural synergies in robot hands via mechanical implementation of principal components analysis, in: Proc. IEEE/RSJ Int. Conf. on Intelligent Robots and Systems, San Diego, 2007, pp. 2877–2882.

[16] D. Prattichizzo, M. Malvezzi, A. Bicchi, On motion and force controllability of grasping hands with postural synergies, in: Proc. of Robotics: Science and Systems, Zaragoza, 2010.

[17] M. Gabiccini, A. Bicchi, On the role of hand synergies in the optimal choice of grasping forces, in: Proc. of Robotics: Science and Systems, Zaragoza, 2010.

[18] D. Prattichizzo, M. Malvezzi, M. Gabiccini, A. Bicchi, On the manipulability ellipsoids of underactuated robotic hands with compliance, Robotics and Autonomous Systems 60 (3) (2012) 337–346.

[19] A. Bicchi, M. Gabiccini, M. Santello, Modelling natural and artificial hands with synergies, Philosophical Transactions of the Royal Society B: Biological Sciences 366 (1581) (2011) 3153–3161.

[20] J. Romero, T. Feix, H. Kjellstrom, D. Kragic, Spatio-temporal modelling of grasping actions, in: Proc. IEEE/RSJ Int. Conf. on Intelligent Robots and Systems, Taipei, 2010, pp. 2103–2108.

[21] A. Tsoli, O. Jenkins, 2d subspaces for user-driven robot grasping, in: Proc. of the RSS 2007 Workshop on Robot Manipulation: Sensing and Adapting to the Real World, Atlanta, 2007.

[22] J. Steffen, R. Haschke, H. Ritter, Towards Dextrous Manipulation Using Manipulation Manifolds, in: Proc. IEEE/RSJ Int. Conf. on Intelligent Robots and Systems, Nice, 2008, pp. 2877–2882.

[23] J. Butterfass, M. Grebenstein, H. Liu, G. Hirzinger, DLR-Hand II: Next generation of a dextrous robot hand, in: Proc. IEEE Int. Conf. on Robotics and Automation, Seoul, 2001.

[24] G. Berselli, G. Borghesan, M. Brandi, C. Melchiorri, C. Natale, G. Palli, S. Pirozzi, G. Vassura, Integrated mechatronic design for a new generation of robotic hands, in: Proc. IFAC Symposium on Robot Control, Gifu, 2009.

[25] G. Palli, C. Melchiorri, G. Vassura, G. Berselli, S. Pirozzi, C. Natale, G. De Maria, C. May, Innovative technologies for the next generation of robotic hands, in: Advanced Bimanual Manipulation, B. Siciliano

(Ed.), Springer Tracts in Advanced Robotics, vol. 80, Springer, 2012, pp. 173–218.

[26] C. Melchiorri, G. Palli, G. Berselli, G. Vassura, On the development of the UB-Hand IV: an overview of design solutions and enabling technologies, IEEE Robotics and Automation Magazine 8 (3) (2013) 72–81.

[27] DEXMART Project website, `http://www.dexmart.eu/`.

[28] L. Biagiotti, F. Lotti, C. Melchiorri, G. Palli, P. Tiezzi, G. Vassura, Development of UB Hand 3: Early results, in: Proc. IEEE Int. Conf. on Robotics and Automation, Barcelona, 2005, pp. 4488–4493.

[29] F. Lotti, G. Vassura, A novel approach to mechanical design of articulated fingers for robotic hands, in: Proc. IEEE/RSJ Int. Conf. on Intelligent Robots and Systems, Lausanne, 2002, pp. 1687–1692.

[30] G. Palli, G. Borghesan, C. Melchiorri, Tendon-based transmission systems for robotic devices: Models and control algorithms, in: Proc. IEEE Int. Conf. on Robotics and Automation, Kobe, 2009, pp. 4063–4068.

[31] G. Palli, G. Borghesan, C. Melchiorri, Friction and visco-elasticity effects in tendon-based transmission systems, in: Proc. IEEE Int. Conf. on Robotics and Automation, Anchorage, 2010, pp. 3890 –3895.

[32] G. Palli, G. Borghesan, C. Melchiorri, Modelling, Identification and Control of Tendon-based Actuation Systems, IEEE Transactions on Robotics 27 (3) (2011) 1–14.

[33] G. Berselli, G. Vassura, Differentiated layer design to modify the compliance of soft pads for robotic limbs, in: Proc. IEEE Int. Conf. on Robotics and Automation, Kobe, 2009, pp. 1285–1290.

[34] G. Berselli, M. Piccinini, G. Vassura, On designing structured soft covers for robotic limbs with predetermined compliance, in: Proc. Int. Design Engineering Technical Conf., Montreal, 2010, pp. 165–174.

[35] G. Berselli, M. Piccinini, G. Palli, G. Vassura, Engineering design of fluid-filled soft covers for robotic contact interfaces: Guidelines, nonlinear modelling, and experimental validation, IEEE Transactions on Robotics 27 (3) (2011) 436–449.

[36] G. Borghesan, G. Palli, C. Melchiorri, Design of tendon-driven robotic fingers: Modelling and control issues, in: Proc. IEEE Int. Conf. on Robotics and Automation, Anchorage, 2010, pp. 793–798.

[37] G. Borghesan, G. Palli, C. Melchiorri, Friction compensation and virtual force sensing for robotic hands, in: Proc. IEEE Int. Conf. on Robotics and Automation, Shanghai, 2011, pp. 4756–4761.

[38] G. Palli, S. Pirozzi, Force Sensor Based on Discrete Optoelectronic Components and Compliant Frames, Sensors And Actuators A: Physical.

[39] G. Palli, S. Pirozzi, Miniaturized optical-based force sensors for tendon-driven robots, in: Proc. IEEE Int. Conf. on Robotics and Automation, Shanghai, 2011, pp. 5344–5349.

[40] G. De Maria, C. Natale, S. Pirozzi, Force/tactile sensor for robotic applications, Sensors and Actuators A: Physical 175 (2012) 60 – 72.

[41] SynGrasp website, `http://www.sirslab.dii.unisi.it/syngrasp/`.

[42] G. Baud-Bovy, J. F. Soechting, Two virtual fingers in the control of the tripod grasp, Journal of Neurophysiology 86 (2) (2001) 604–615.